Journal of
Mechanics of
Materials and Structures

NUMERICAL INVESTIGATION OF DIRECTOR ORIENTATION AND FLOW OF NEMATIC LIQUID CRYSTALS IN A PLANAR 1:4 EXPANSION

Pedro A. Cruz, Murilo F. Tomé, Iain W. Stewart and Sean McKee

Volume 6, No. 7-8 September–October 2011

mathematical sciences publishers

JOURNAL OF MECHANICS OF MATERIALS AND STRUCTURES
Vol. 6, No. 7-8, 2011

msp

NUMERICAL INVESTIGATION OF DIRECTOR ORIENTATION AND FLOW OF NEMATIC LIQUID CRYSTALS IN A PLANAR 1:4 EXPANSION

PEDRO A. CRUZ, MURILO F. TOMÉ, IAIN W. STEWART AND SEAN MCKEE

Numerical solutions to the equations describing Ericksen–Leslie dynamic theory for 2D nematic liquid crystal flows subject to a magnetic field are obtained. The governing equations are solved by a finite difference technique based on the GENSMAC methodology. The resulting numerical technique was verified by comparing numerical solutions for 2D-channel flow by means of mesh refinement. To demonstrate the capabilities of this method, the flow of a nematic liquid crystal in a planar 1:4 expansion was simulated. Calculations were performed for various Ericksen and Reynolds numbers. The results showed that an increase in the Ericksen number caused the appearance of lip and corner vortices.

1. Introduction

Although the discovery of liquid crystals is generally attributed to Reinitzer [1888], the term "liquid crystal" was established by Lehmann in 1900, after he originally suggested the term "flowing crystals" [Lehmann 1889]. In [Friedel 1922] different liquid crystal phases were described and three broad categories were proposed: nematic, cholesteric, and smectic. Nematic liquid crystals are characterized by long-range orientational order of the molecules; in other words, the molecular orientation in a nematic liquid crystal exhibits a preferred direction which can be represented by a unit vector $\boldsymbol{n}$, called the director. Gray et al. [1973; 1974] synthesized a nematic liquid crystal that was stable at room temperature and so could be used in display monitors, known as liquid crystal displays; since then, nematic liquid crystals have been rather attractive owing to their applications in high-performance optoelectronic products and their striking rheological properties.

The basic theory that describes the dynamics of nematic liquid crystals is the Ericksen–Leslie dynamic theory, proposed by [Ericksen 1961; Leslie 1966; 1968]. This theory has consistently been applied to many flow problems of nematic liquid crystals, but the equations are complex so that analytic solutions of nematic liquid crystals flows are extremely rare. Consequently, numerical methods are becoming an important tool for solving these highly nonlinear equations.

Many articles treating the flow of nematic liquid crystals can be found (see, for example, [Pieranski and Guyon 1974; Baleo et al. 1992; Chono and Suji 1998; Chono et al. 1998; Carou et al. 2006]). For instance, in [Baleo et al. 1992] elasticity was neglected, in which case the equations reduce to the Ericksen transversely isotropic fluids. In [Chono et al. 1998] the spatial development of the director orientation was studied in tumbling nematic liquid crystals in channel flow. In [Chono and Suji 1998] the flow

This work was supported by FAPESP grant number 07/07038-2, CNPq grants numbers 304422/2007-0 and 470764/2007-4, and CAPES grants numbers 4897/09-9 and 2844/10-9. This work was carried out in the framework of the INCT-MACC (CNPq, Brazil).

Keywords: nematic liquid crystal, Ericksen–Leslie equations, two-dimensional flow, finite difference.

around a circular cylinder was analyzed. In other studies, such as [Pieranski and Guyon 1974], the investigation was through experimentation. However, to our knowledge, studies using the full Ericksen–Leslie equations for 2D flows are extremely rare.

This paper presents a finite difference technique for solving the full Ericksen–Leslie dynamic equations in two dimensions under the influence of a finite magnetic field.

2. Governing equations

We consider the 2D flow of nematic liquid crystals. A magnetic field is applied and we assume the one-constant approximation for the elastic constants. The unitary director $\boldsymbol{n}$ and velocity $\boldsymbol{v}$ can be written as

$$\boldsymbol{n} = (\cos\phi, \sin\phi, 0), \qquad \phi = \phi(x, y, t), \tag{2-1}$$

$$\boldsymbol{v} = \big(u(x, y, t), v(x, y, t), 0\big), \tag{2-2}$$

where ϕ is the orientation angle of the director. The magnetic field potential (equal to the negative of the magnetic energy) is

$$\Psi = \tfrac{1}{2}\mu_0 \Delta\chi (\boldsymbol{n}\cdot\boldsymbol{H})^2, \qquad \boldsymbol{H} = H(\cos\phi_0, \sin\phi_0, 0), \qquad |\boldsymbol{H}| = H < \infty, \tag{2-3}$$

where $\Delta\chi > 0$ is the magnetic anisotropy, H is the magnitude of the field, and ϕ_0 is a constant. The related external generalized body force G_i is given by

$$G_i = \frac{\partial\Psi}{\partial n_i} = \mu_0\Delta\chi(\boldsymbol{n}\cdot\boldsymbol{H})H_i, \tag{2-4}$$

where $\mu_0 > 0$ is the permeability of free space.

We shall use the usual Einstein summation convention where appropriate. A comma indicates partial differentiation with respect to the variable it precedes; for example $n_{i,j}$ denotes the partial derivative of the i-th component of n_i with respect to the j-th variable.

The basic equations for simulating 2D flows of a nematic liquid crystal are the conservation of mass, elastic energy, linear momentum, and angular momentum, which can be written, respectively, in dimensionless form as follows (for details see [Cruz et al. 2010]):

$$u_{,x} + v_{,y} = 0, \tag{2-5}$$

$$(w_F)_{,x} = \frac{1}{\mathrm{Re}\,\mathrm{Er}}[\phi_{,xx} + (\phi_{,y})_{,x}], \qquad (w_F)_{,y} = \frac{1}{\mathrm{Re}\,\mathrm{Er}}[(\phi_{,x})_{,y} + \phi_{,yy}], \tag{2-6}$$

$$u_{,t} = -(uu)_{,x} - (vu)_{,y} - p_{,x} - w_{F,x} + R_j n_{j,x} + \frac{1}{\mathrm{Re}}\big[\tfrac{1}{2}\alpha_4(u_{,xx} + u_{,yy}) + \Phi_{xx,x} + \Phi_{xy,y}\big] + \tfrac{1}{2}\mu_0\Delta\chi H^2 \sin(2(\phi_0 - \phi))\phi_{,x}, \tag{2-7}$$

$$v_{,t} = -(uv)_{,x} - (vv)_{,y} - p_{,y} - w_{F,y} + R_j n_{j,y} + \frac{1}{\mathrm{Re}}\big[\tfrac{1}{2}\alpha_4(v_{,xx} + v_{,yy}) + \Phi_{yx,x} + \Phi_{yy,y}\big] + \tfrac{1}{2}\mu_0\Delta\chi H^2 \sin(2(\phi_0 - \phi))\phi_{,y}, \tag{2-8}$$

$$\phi_{,t} = -(u\phi)_{,x} - (v\phi)_{,y} + \frac{1}{\mathrm{Er}\,\gamma_1}[\phi_{,xx} + \phi_{,yy}] - \frac{\gamma_2}{2\gamma_1}\big[(u_{,y} + v_{,x})\cos(2\phi) + (v_{,y} - u_{,x})\sin(2\phi)\big] - \tfrac{1}{2}(u_{,y} - v_{,x}) - \frac{\mathrm{Re}}{2\gamma_1}\mu_0\Delta\chi H^2 \sin(2(\phi_0 - \phi)), \tag{2-9}$$

where $\mathrm{Re} = \rho UL/\eta$ and $\mathrm{Er} = UL(\eta/K)$ are the Reynolds and Ericksen numbers, respectively. The coefficient $\gamma_1 = \alpha_3 - \alpha_2 \geq 0$ is often referred to as the twist or rotational viscosity and the coefficient $\gamma_2 = \alpha_2 + \alpha_3 = \alpha_6 - \alpha_5$ is called the torsion coefficient. The viscosities $\alpha_1, \alpha_2, \ldots, \alpha_6$ are the Leslie viscosities.

The functions $\Phi_{xx}, \ldots, \Phi_{yy}$ are given by

$$\begin{aligned}\Phi_{xx} = {} & \alpha_1 \cos^2\phi\big(u_{,x}\cos^2\phi + v_{,y}\sin^2\phi + \tfrac{1}{2}(u_{,y}+v_{,x})\sin(2\phi)\big) \\ & - (\alpha_2+\alpha_3)\sin\phi\cos\phi\big(\phi_{,t} + u\phi_{,x} + v\phi_{,y} + \tfrac{1}{2}(u_{,y}-v_{,x})\big) \\ & + (\alpha_5+\alpha_6)\big(u_{,x}\cos^2\phi + \tfrac{1}{2}\sin\phi\cos\phi\,(u_{,y}+v_{,x})\big), \end{aligned} \tag{2-10}$$

$$\begin{aligned}\Phi_{xy} = {} & \alpha_1 \sin\phi\cos\phi\big(u_{,x}\cos^2\phi + v_{,y}\sin^2\phi + \tfrac{1}{2}(u_{,y}+v_{,x})\sin(2\phi)\big) \\ & + (\alpha_3\cos^2\phi - \alpha_2\sin^2\phi)\big(\phi_{,t} + u\phi_{,x} + v\phi_{,y} + \tfrac{1}{2}(u_{,y}-v_{,x})\big) \\ & + \tfrac{1}{2}(\alpha_5\sin^2\phi + \alpha_6\cos^2\phi)(u_{,y}+v_{,x}) + (\alpha_5 u_{,x} + \alpha_6 v_{,y})\sin\phi\cos\phi, \end{aligned} \tag{2-11}$$

$$\begin{aligned}\Phi_{yx} = {} & \alpha_1 \sin\phi\cos\phi\big(u_{,x}\cos^2\phi + v_{,y}\sin^2\phi + \tfrac{1}{2}(u_{,y}+v_{,x})\sin(2\phi)\big) \\ & + (\alpha_2\cos^2\phi - \alpha_3\sin^2\phi)\big(\phi_{,t} + u\phi_{,x} + v\phi_{,y} + \tfrac{1}{2}(u_{,y}-v_{,x})\big) \\ & + \tfrac{1}{2}(\alpha_5\cos^2\phi + \alpha_6\sin^2\phi)(u_{,y}+v_{,x}) + (\alpha_5 v_{,y} + \alpha_6 u_{,x})\sin\phi\cos\phi, \end{aligned} \tag{2-12}$$

$$\begin{aligned}\Phi_{yy} = {} & \alpha_1 \sin^2\phi\big(u_{,x}\cos^2\phi + v_{,y}\sin^2\phi + \tfrac{1}{2}(u_{,y}+v_{,x})\sin(2\phi)\big) \\ & + (\alpha_2+\alpha_3)\sin\phi\cos\phi\big(\phi_{,t} + u\phi_{,x} + v\phi_{,y} + \tfrac{1}{2}(u_{,y}-v_{,x})\big) \\ & + (\alpha_5+\alpha_6)\big(v_{,y}\sin^2\phi + \tfrac{1}{2}\sin\phi\cos\phi\,(u_{,y}+v_{,x})\big). \end{aligned} \tag{2-13}$$

The terms $R_j n_{j,x}$ and $R_j n_{j,y}$ are given by

$$\begin{aligned}R_j n_{j,x} = {} & \frac{1}{\mathrm{Re}}\big\{-\gamma_1\phi_{,x}\big(\phi_{,t} + u\phi_{,x} + v\phi_{,y} + \tfrac{1}{2}(u_{,y}-v_{,x})\big) \\ & - \tfrac{1}{2}\big(\gamma_2\phi_{,x}\cos(2\phi)(u_{,y}+v_{,x}) + \gamma_2\phi_{,x}\sin(2\phi)(u_{,x}-v_{,y})\big)\big\}, \end{aligned} \tag{2-14}$$

$$\begin{aligned}R_j n_{j,y} = {} & \frac{1}{\mathrm{Re}}\big\{-\gamma_1\phi_{,y}\big(\phi_{,t} + u\phi_{,x} + v\phi_{,y} + \tfrac{1}{2}(u_{,y}-v_{,x})\big) \\ & - \tfrac{1}{2}\big(\gamma_2\phi_{,y}\cos(2\phi)(u_{,y}+v_{,x}) + \gamma_2\phi_{,y}\sin(2\phi)(u_{,x}-v_{,y})\big)\big\}. \end{aligned} \tag{2-15}$$

In these equations, the viscosities $\alpha_1, \ldots, \alpha_6$ have been scaled by the factor $\eta = \alpha_3 - \alpha_2$.

Equations (2-5) and (2-7)–(2-9) form the complete set of dynamic equations and must be solved subject to suitable boundary conditions in order to find solutions for ϕ, p, u, and v.

2A. ***Boundary conditions.*** To solve (2-5) and (2-7)–(2-9) we impose the following boundary conditions for the velocity field. On rigid boundaries we set $v_i = 0$ while at fluid entrances (inflows) the normal velocity is specified by $v_{\mathrm{N}} = V_{\mathrm{inf}}$ and the tangential velocity by $v_{\mathrm{T}} = 0$. Here N denotes normal direction to the boundary and T denotes the tangential direction. At fluid exits (outflows) the Neumann condition $v_{i,\mathrm{N}} = 0$ is adopted.

The director is strongly anchored on rigid walls. This means that the anchoring angle is set according to the orientation of the rigid wall. Details of this anchoring angle will be given in the section dealing

with numerical results. The choice of the angle of the director at fluid entrances (inflows) is $\phi = 0$, and at fluid exits (outflows) we set $\phi_{,\mathrm{N}} = 0$.

2B. ***Numerical procedure.*** The numerical method is a standard and robust approach using Chorin's projection method. An interesting but different method was employed in [Svenšek and Žumer 2002]. The momentum equations (2-7) and (2-8), the mass conservation equation (2-5), and the angular momentum equation (2-9) will be solved by a methodology based on the algorithm introduced in [Tomé et al. 2002] as follows.

Assume that, at time t_n, the velocity field $v_i(x_k, t_n)$ and the orientation angle of the director $\phi(x_k, t_n)$ are known and that suitable boundary conditions are provided. To calculate the velocity field $v_i(x_k, t_{n+1})$, the pressure $p(x_k, t_{n+1})$, the functions $\Phi_{ij}(x_k, t_{n+1})$, and the orientation angle of the director $\phi(x_k, t_{n+1})$, we proceed in the following manner:

Step 1. Using the values of $v_i(x_k, t_n)$ and $\phi(x_k, t_n)$, solve (2-6) for $w_F(x_k, t_n)$ and calculate $w_{F,i}(x_k, t_n)$, $\Phi_{ij}(x_k, t_n)$, and $R_j n_{j,i}(x_k, t_n)$ from (2-10)–(2-13), (2-14) and (2-15), respectively.

Step 2. Calculate an intermediate velocity field $\tilde{v}_i(x_k, t_{n+1})$ from

$$\frac{\partial \tilde{v}_i}{\partial t} = -(v_j v_i)_{,j} - w_{F,i} + R_j n_{j,i} + \tfrac{1}{2}\mu_0 \Delta\chi H^2 \sin(2(\phi_0 - \phi))\phi_{,i} + \frac{1}{\mathrm{Re}}\left[\tfrac{1}{2}\alpha_4 (v_{i,j})_{,j} + \Phi_{ij,j}\right], \quad (2\text{-}16)$$

with $\tilde{v}_i(x_k, t_n) = v_i(x_k, t_n)$ using the same boundary conditions for the velocity $v_i(x_k, t_n)$. This equation is solved by an explicit finite difference method. In [Tomé et al. 1996] it was shown that $\tilde{v}_i$ possesses the correct vorticity at time t_{n+1}.

Step 3. Solve the Poisson equation

$$\psi_{,ii}(x_k, t_{n+1}) = \tilde{v}_{i,i}(x_k, t_{n+1}), \quad (2\text{-}17)$$

subject to the boundary conditions that $\psi_{,N} = 0$ on rigid boundaries and inflows and $\psi = 0$ on outflows [Tomé and McKee 1994].

Step 4. Calculate the final velocity field:

$$v_i(x_k, t_{n+1}) = \tilde{v}_i(x_k, t_{n+1}) - \psi_{,i}(x_k, t_{n+1}). \quad (2\text{-}18)$$

Step 5. Determine the pressure field $p(x_k, t_{n+1})$ [Tomé et al. 1996]:

$$p(x_k, t_{n+1}) = \frac{\psi(x_k, t_{n+1})}{\delta t}. \quad (2\text{-}19)$$

Step 6. Calculate the angle of the director $\phi(x_k, t_{n+1})$ from (2-9). This equation is solved by an explicit finite difference method.

Step 7. Calculate the functions $\Phi_{ij}(x_k, t_{n+1})$ from (2-10).

3. Approximation of the equations by finite differences

The equations contained in the numerical procedure outlined in the previous section are solved by the finite difference method as follows. A staggered grid is employed. This was first introduced in [Harlow and Welch 1965]; it has been used by many investigators because it locally guarantees conservation of mass and momentum while remaining computationally simple.

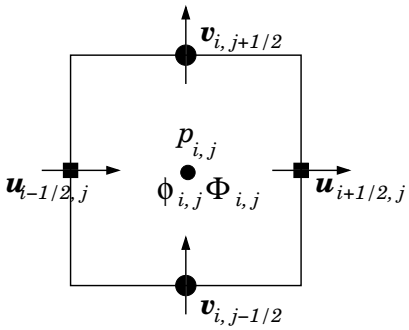

Figure 1. 2D staggered cell.

The velocities u and v are located at the middle of cell faces while the other quantities (ϕ, Φ, p, w_F) are positioned at cell centers. Figure 1 illustrates a typical 2D cell of dimensions $\delta x \times \delta y$.

The momentum conservation equations (2-7) and (2-8) and the angular momentum equation (2-9) are solved by the explicit Euler method. The spatial derivatives in the momentum conservation equations are discretized at points $\left((i+\frac{1}{2})\delta x,\, j\delta y\right)$ and $\left(i\delta x,\, (j+\frac{1}{2})\delta y\right)$ while the angular momentum equation (2-9), the density of elastic energy (2-6), and the functions Φ_{ij} are approximated at cell centers $(i\delta x,\, j\delta y)$. The divergence of Φ_{ij}, the gradient of the density of elastic energy $w_{F,i}$, and the terms $R_j n_{j,i}$ are approximated by central differences.

For reasons of space, the details of the finite differences equations involved are not presented here; they can be found in [Cruz et al. 2010].

4. Validation results

The numerical method described in the previous sections was applied to simulate the flow of the nematic liquid crystal MBBA at 25° C. We considered a 2D-channel (see Figure 2) with width L and length $C = 10L$. The boundary conditions for the velocity field were those specified in Section 2A. At the fluid entrance, a fully developed flow was applied:

$$u(y) = -4\frac{U}{L}\left(y - \frac{L}{2}\right)^2 + U, \tag{4-1}$$

where U is a prescribed value for velocity.

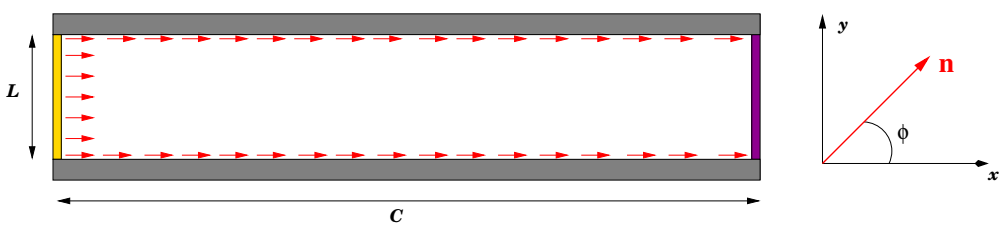

Figure 2. Definition of the domain for the simulation of the flow in a 2D channel. The red arrows indicate the boundary conditions used for the calculation of the angle ϕ by means of (2-9).

Leslie viscosities	α_1	α_2	α_3	α_4	α_5	α_6
MBBA near 25° C	−0.0181	−0.1104	−0.001104	0.0826	0.0779	−0.0336
MBBA near 42° C	−0.0036	−0.0310	−0.00218	0.0394	0.0224	−0.01086

Table 1. Leslie viscosities for the nematic liquid crystal MBBA, in SI units [Stewart 2004].

Physical parameter	$\Delta\chi$	ρ	μ_0	K
Values	1.219×10^{-6}	$1088\,\mathrm{kg\,m^{-3}}$	$12.566 \times 10^{-7}\,\mathrm{H\,m^{-1}}$	$7.5 \times 10^{-12}\,\mathrm{N}$

Table 2. Physical parameters for the nematic phases of MBBA, in SI units: magnetic anisotropy ($\Delta\chi$, unitless) [Stephen and Straley 1974], density (ρ) [Stephen and Straley 1974; Stewart 2004], permeability of free space (μ_0), and elastic constant (K). The viscosities at 42° C were taken from [Kneppe et al. 1982].

To simulate this problem, the following input data (specifying the flow) were employed:

- Width of the entry plane $L = 0.001$ m and velocity scale $U = 0.00038\,\mathrm{m\,s^{-1}}$.

A magnetic field $H = 1/(4\pi)10^3\,\mathrm{A\,m^{-1}}$ was applied. The physical parameters, specifying the nematic liquid crystal MBBA at 25°, are given in Tables 1 and 2. With these data we obtain $\mathrm{Re} = 0.0038$ and $\mathrm{Er} = 55.38$. To demonstrate the convergence of the numerical method presented in this paper, we simulated channel flow using four embedded meshes until steady state was achieved. The meshes employed were:

- M_0: $\delta x = \delta y = 0.000125$ m (80×8 cells),
- M_1: $\delta x = \delta y = 0.0000625$ m (160×16 cells),
- M_2: $\delta x = \delta y = 0.00003125$ m (320×32 cells), and
- M_3: $\delta x = \delta y = 0.000015625$ m (640×64 cells).

An analytic solution for this problem is not known, so we compared the solutions obtained on meshes M_0, M_1, and M_2 to the solution obtained on the finest mesh, M_3, which we refer to here to as "exact".

Figure 3 displays the numerical and the "exact" values of $u(y)$ at the end of the channel ($x = 10L$). We can see that there is good agreement between the solutions. Moreover, Figure 3 shows that as the mesh is refined the numerical solutions tend to the "exact" solution. Similar results were obtained for the functions Φ_{xx}, Φ_{xy}, Φ_{yx}, and Φ_{yy}. These results suggest that the numerical method presented in this work is convergent.

5. Numerical investigation of nematic liquid crystal flow in a planar 1:4 expansion

In this section we present numerical results from the simulation of the flow of a nematic liquid crystal through a planar 1:4 expansion as illustrated in Figure 4. In this problem, the fluid flows from a channel with width $2L$ into another channel having width $8L$.

This problem is one of the classic benchmarks employed in the study of the development of numerical methods for simulating non-Newtonian fluids. The interest in simulations of this kind of flow comes from the fact that non-Newtonian fluids exhibit a variety of phenomena. A particular point of interest is

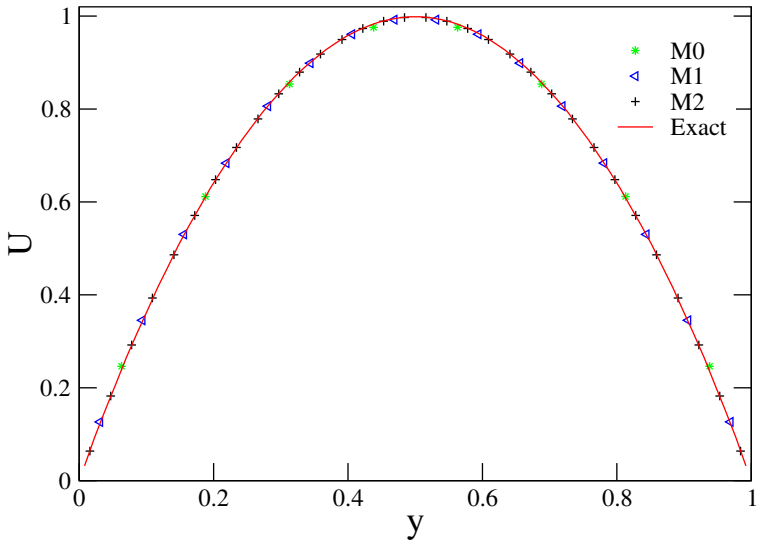

Figure 3. Numerical simulation of channel flow: Re = 0.0038 and Er = 55.38. Comparison between the "exact" and the numerical solutions of $u(y)$ at $x = 10L$.

the study of the behavior of vortices in the corners, and vortices that are generated near the expansion entrance (known as lip vortices). The length and intensity of these vortices can be affected by both the Ericksen and Reynolds numbers and the type of expansion as well as by rheological properties of the material such as viscosity and elastic constants.

The boundary conditions for the velocity field were those specified in Section 2A while at the channel entrance the velocity was specified by the fully developed profile given by (4-1).

Boundary conditions for the angle ϕ. The boundary conditions for the angle ϕ were specified as follows (for details see Figure 4):

(1) Along the horizontal walls, the anchoring angle was set to zero, implying parallel alignment to the walls.

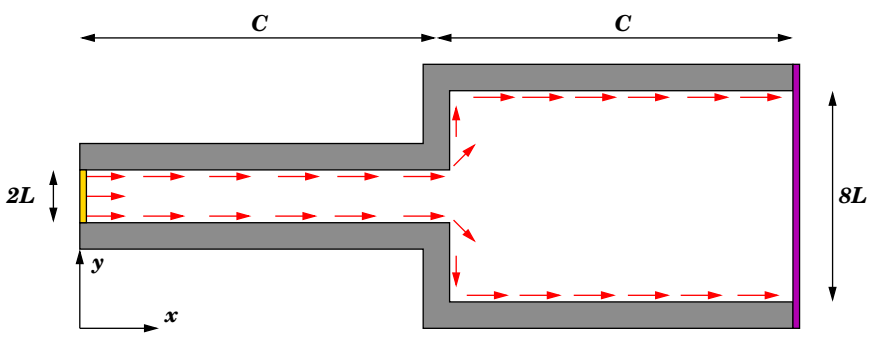

Figure 4. Definition of the domain for the simulation of the flow in a 1:4 expansion. The red arrows indicate the boundary conditions used for the calculation of the angle ϕ by (2-9).

(2) At the expansion entrance, we used:
   (a) $\phi = 45°$ (upper lip corner in Figure 4);
   (b) $\phi = -45°$ (lower lip corner in Figure 4).

(3) On the vertical walls (or the expansion walls), we employed:
   (a) $\phi = -90°$ at $x = C$ and $0 \le y \le 3L$;
   (b) $\phi = 90°$ at $x = C$ and $5L \le y \le 8L$.

(4) At the channel entry defined by $x = 0$ and $3L \le y \le 5L$, we set $\phi = 0$ and at the exit plane, $x = 2C$ and $0 \le y \le 8L$, we assumed $\phi_{,x} = 0$.

The relevant physical parameters specific to the nematic liquid crystal MBBA at 25° and 42° are presented in Tables 1 and 2, respectively. The remaining parameters specifying the flow were:

- viscosity scales: $\eta_{25°} = \alpha_3 - \alpha_2 = 0.109296\,\text{Pa}\cdot\text{s}$ and $\eta_{42°} = \alpha_3 - \alpha_2 = 0.02882\,\text{Pa}\cdot\text{s}$;
- mesh (**M**): 200×40 cells ($\delta x = \delta y = 0.0001$ m);
- width of the entry plane: $2L = 0.001$ m;

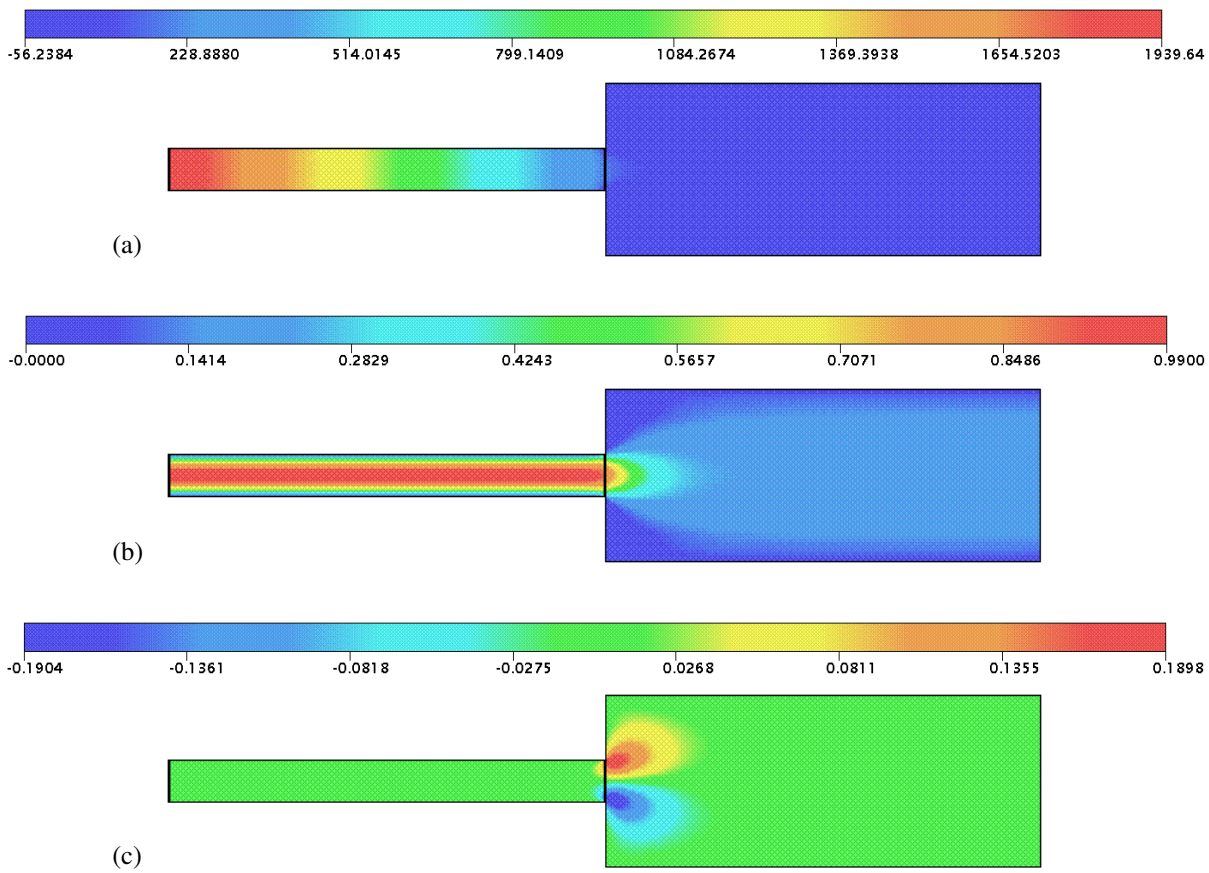

Figure 5. Numerical simulation of the flow in a planar 1:4 expansion with $\text{Re} = 0.005$ and $\text{Er} = 7.2$ at $t = 40$ s. Isolines: (a) pressure, (b) velocity u, and (c) velocity v.

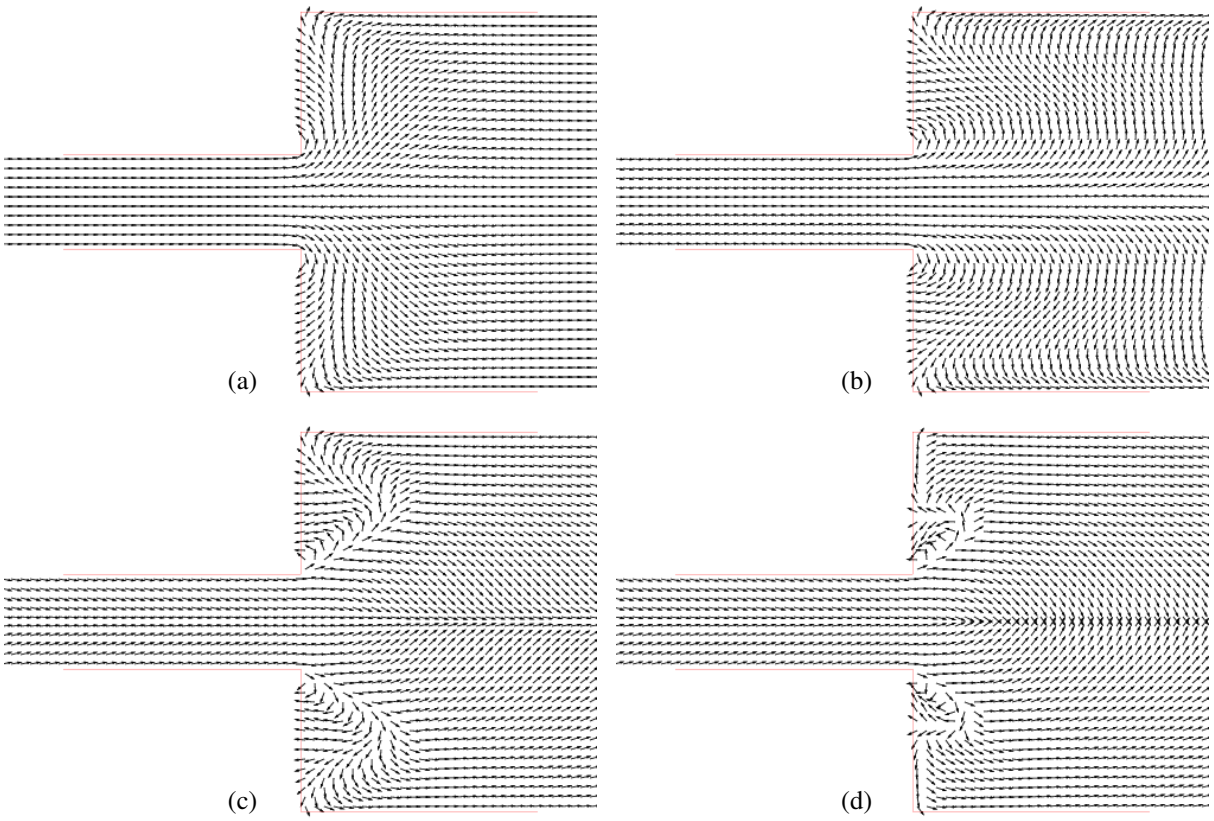

Figure 6. Plots of director with Re = 0.019 for different Ericksen numbers: (a) Er = 1.9, (b) Er = 19.2, (c) Er = 192, and (d) Er = 1920.

- length of the channels: $C = 0.01\,\mathrm{m}$;
- width of the exit plane: $8L = 0.004\,\mathrm{m}$;
- velocity at the entry channel: $V_{\mathrm{inf}} = 0.00025\,\mathrm{m\,s^{-1}}$;
- velocity scale: $U = 0.001\,\mathrm{m\,s^{-1}}$;
- length scale: $L = 0.0005\,\mathrm{m}$.

The Reynolds number was calculated using the half-width L of the channel entrance, the velocity scale $U = 0.001\,\mathrm{m\,s^{-1}}$, and the viscosity scales η_{25° and η_{42° were selected so that Re = 0.005 and Re = 0.019, respectively. In the results that follow the following Ericksen numbers ($\mathrm{Er} = UL\eta/K$) were employed:

$$\mathrm{Re} = 0.005 \begin{cases} K = 7.5 \times 10^{-9} & \Longrightarrow \quad \mathrm{Er} = 7.2, \\ K = 7.5 \times 10^{-10} & \Longrightarrow \quad \mathrm{Er} = 72.8, \\ K = 7.5 \times 10^{-11} & \Longrightarrow \quad \mathrm{Er} = 728, \\ K = 7.5 \times 10^{-12} & \Longrightarrow \quad \mathrm{Er} = 7286, \end{cases}$$

$$\mathrm{Re} = 0.019 \begin{cases} K = 7.5 \times 10^{-9} & \Longrightarrow \quad \mathrm{Er} = 1.9, \\ K = 7.5 \times 10^{-10} & \Longrightarrow \quad \mathrm{Er} = 19.2, \\ K = 7.5 \times 10^{-11} & \Longrightarrow \quad \mathrm{Er} = 192, \\ K = 7.5 \times 10^{-12} & \Longrightarrow \quad \mathrm{Er} = 1920. \end{cases}$$

To observe elastic and viscous effects in the flow, such as the appearance of corner and lip vortices, we simulated this problem for the values of the Reynolds and Ericksen numbers given above until a steady state was reached. Each simulation was performed until $t = 40\,\mathrm{s}$. Figure 5 displays the isolines of pressure and velocity at time $t = 40\,\mathrm{s}$ for $\mathrm{Re} = 0.005$ and $\mathrm{Er} = 7.2$. From Figure 5 one can see that the pressure only varies in the x-direction and the velocity is parabolic within the entrance channel so we can conclude that the steady state has been reached.

A zoom-in on the solutions obtained for the director and the streamlines near the expansion entrance for the case $\mathrm{Re} = 0.019$ is displayed in Figures 6 and 7 while Figures 8 and 9 show the results obtained with $\mathrm{Re} = 0.005$.

For $\mathrm{Er} = 1.9, 19.2$ (see Figures 6a and 6b) the director profile did not display a great deal of variation: at the centerline the vectors are parallel while away from it, the vectors are diverging pointing to the expansion walls. For $\mathrm{Er} = 192$ we can observe significant disturbances in the director profile where one

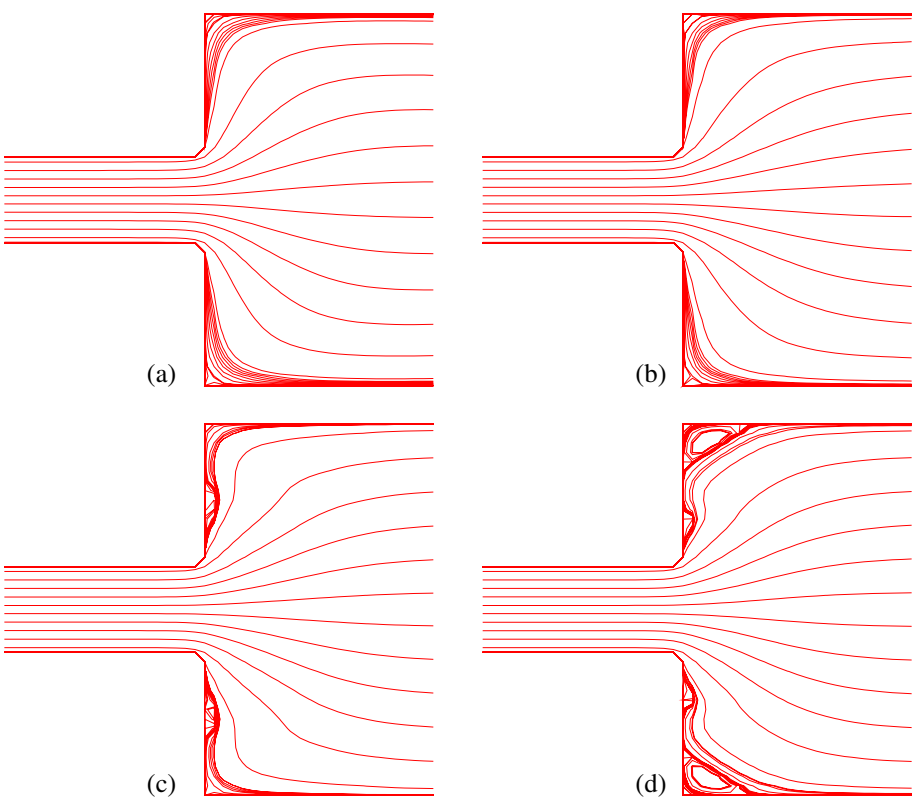

Figure 7. Plots of streamlines with $\mathrm{Re} = 0.019$ for different Ericksen numbers: (a) $\mathrm{Er} = 1.9$, (b) $\mathrm{Er} = 19.2$, (c) $\mathrm{Er} = 192$, and (d) $\mathrm{Er} = 1920$.

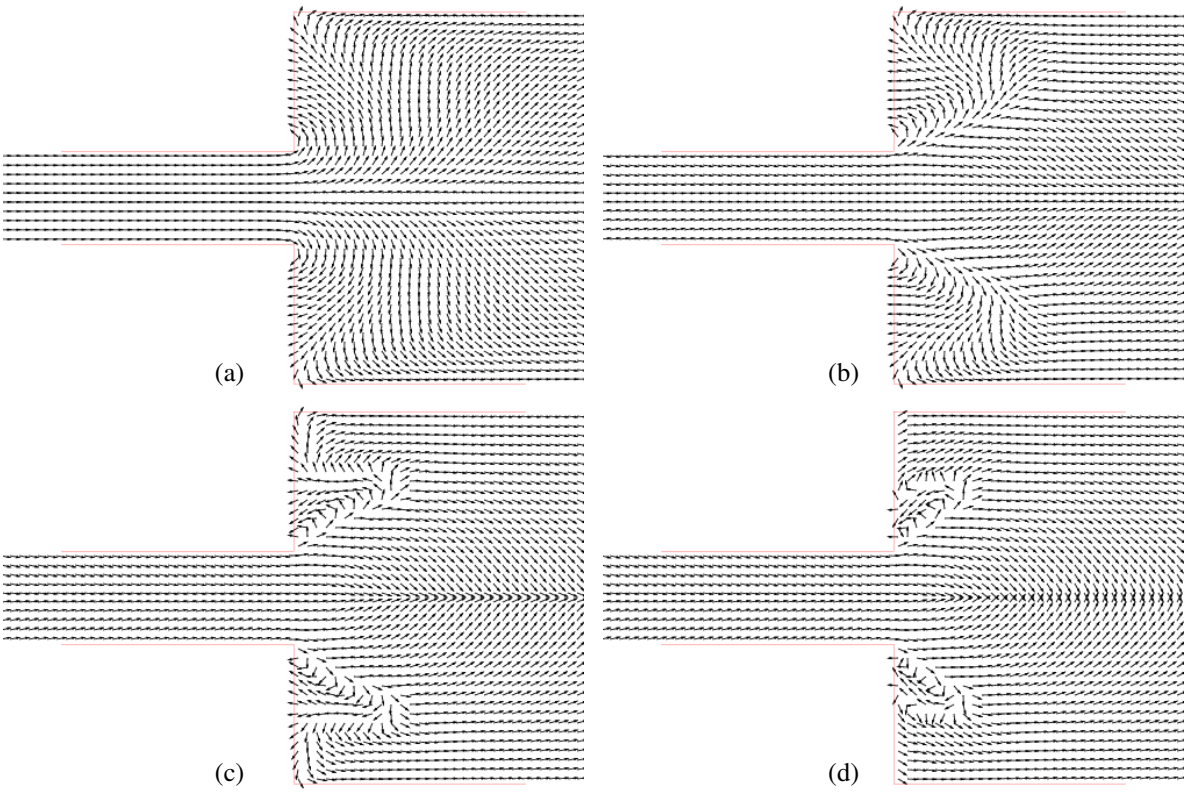

Figure 8. Plots of director with Re = 0.005 for different Ericksen numbers: (a) Er = 7.2, (b) Er = 72.8, (c) Er = 728, and (d) Er = 7286.

can see the appearance of a small lip vortex (see Figure 6c). Near the symmetry axis, we can see that the director is converging to the centerline. For Er = 1920 (see Figure 6d), the director, at the symmetry axis, is perpendicular to the centerline. We now observe a larger lip vortex concentrated near the entrance of the expansion walls.

The corresponding streamlines displayed in Figure 7 are interesting since they display a lip vortex for Er = 192, 1920 (see Figures 7c and 7d). As the Ericksen number is increased to Er = 1920 a large corner vortex is generated. These results show that the appearance of the lip and corner vortices were caused by an increase in the Ericksen number. This phenomenon is similar to that observed by many authors in certain viscous anisotropic fluids through a 4:1 contraction (for example, [Yoo and Na 1991; Nigen and Walters 2002; Alves et al. 2003]) where the corner vortex decreases with increasing elasticity. The results obtained with Re = 0.005 were similar to those obtained with Re = 0.019 except that the lip vortex appears first at the smaller Ericksen number of Er = 72.8. The occurrence of the corner vortex is also anticipated (see Figure 9b). Tables 3 and 4 display the size of vortices obtained for each value of the Ericksen number employed in the simulations. We see in these tables that the size of the corner vortices encountered for Re = 0.005 are larger than those obtained with Re = 0.019. We believe that the appearance of larger corner vortices in the case Re = 0.005 was due to viscous and elastic forces associated with a smaller Re and higher Er.

Er	1.9	19.2	192	1920
length	0.0000	0.0000	0.1000	1.441506

Table 3. Length of the corner vortices as a function of the Ericksen number for Re = 0.019.

Er	7.2	72.8	728	7280
length	0.0000	0.0500	0.618543	1.738053

Table 4. Length of the corner vortices as a function of the Ericksen number for Re = 0.005.

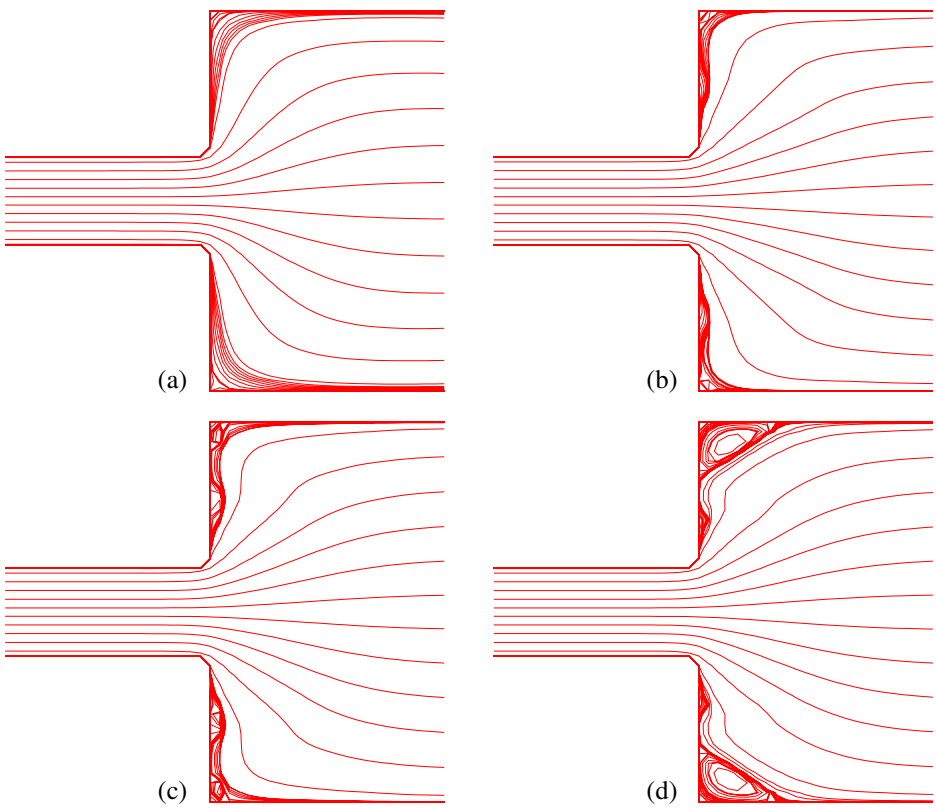

Figure 9. Plots of streamlines with Re = 0.005 for different Ericksen numbers: (a) Er = 7.2, (b) Er = 72.8, (c) Er = 728, and (d) Er = 7286.

6. Conclusions

This paper has dealt with the development of a numerical method for simulating 2D flows of nematic liquid crystals described by the Ericksen–Leslie equations. The numerical technique was based on the method developed in [Tomé et al. 2002] and used the finite difference method. The validation of the technique was performed through the simulation of the flow in a channel using four refined meshes: M_0, M_1, M_2, and M_3. An analytic solution for this problem is not yet available, so we compared the solutions

obtained on meshes M_0, M_1, and M_2 to the solution obtained on the finest mesh M_3, which we called "exact". Good agreement was obtained between the numerical solutions on the coarser meshes and the solution on mesh M_3. We then applied the numerical technique to simulate the flow through a planar 1:4 expansion for various values of the Ericksen number. The results showed that as the Ericksen number is increased interesting effects were observed: the orientation of the director displayed the appearance of a lip vortex while increasing the Ericksen number had the effect of producing a lip vortex at the entrance of the expansion. Increasing the Ericksen number further resulted in the appearance of a corner vortex that increased in size with increasing Ericksen number. The results showed that both elasticity and viscosity had a considerable effect on the formation of corner and lip vortices.

References

[Alves et al. 2003] M. A. Alves, P. J. Oliveira, and F. T. Pinho, "Numerical simulation of viscoelastic contraction flows", pp. 826–829 in *Computational fluid and solid mechanics*, edited by K. Bathe, Elsevier, Amsterdam, 2003.

[Baleo et al. 1992] J. N. Baleo, M. Vincent, P. Navard, and Y. Demay, "Finite element simulation of flow and director orientation of viscous anisotropic fluids in complex 2D geometries", *J. Rheol.* **36**:4 (1992), 663–701.

[Carou et al. 2006] J. Q. Carou, B. R. Duffy, N. J. Mottram, and S. K. Wilson, "Shear-driven and pressure-driven flow of a nematic liquid crystal in a slowly varying channel", *Phys. Fluids* **18**:2 (2006), article ID 027105.

[Chono and Suji 1998] S. Chono and T. Suji, "Numerical simulation of nematic liquid crystalline flows around a circular cylinder", *Mol. Cryst. Liq. Cryst.* **309** (1998), 217–236.

[Chono et al. 1998] S. Chono, T. Tsuji, and M. M. Denn, "Spatial development of director orientation of tumbling nematic liquid crystals in pressure-driven channel flow", *J. Non-Newton. Fluid Mech.* **79**:2–3 (1998), 515–527.

[Cruz et al. 2010] P. A. Cruz, M. F. Tomé, I. W. Stewart, and S. McKee, "Numerical solution of the Ericksen–Leslie dynamic equations for two-dimensional nematic liquid crystal flows", Report 21, Department of Mathematics and Statistics, University of Strathclyde, Glasgow, 2010.

[Ericksen 1961] J. L. Ericksen, "Conservation laws for liquid crystals", *J. Rheol.* **5**:1 (1961), 23–34.

[Friedel 1922] G. Friedel, "Les états mésomorphes de la matière", *Annales Physique* (*Paris*) **18** (1922), 273–474.

[Gray et al. 1973] G. W. Gray, K. J. Harrison, and J. A. Nash, "New family of nematic liquid crystals for displays", *Electron. Lett.* **9**:6 (1973), 130–131.

[Gray et al. 1974] G. W. Gray, K. J. Harrison, J. A. Nash, J. Constant, D. S. Hulme, J. Kirton, and E. P. Raynes, "Stable, low melting nematogens of positive dielectric anisotropy for display devices", pp. 617–643 in *Liquid crystals and ordered fluids*, vol. 2, edited by J. F. Johnson and R. S. Porter, Plenum Press, New York, 1974.

[Harlow and Welch 1965] F. H. Harlow and J. E. Welch, "Numerical calculation of time-dependent viscous incompressible flow of fluid with free surface", *Phys. Fluids* **8**:12 (1965), 2182–2189.

[Kneppe et al. 1982] H. Kneppe, F. Schneider, and N. K. Sharma, "Rotational viscosity γ_1 of nematic liquid crystals", *J. Chem. Phys.* **77**:6 (1982), 3203–3208.

[Lehmann 1889] O. Lehmann, "Über fliessende Krystalle", *Zeitschrift für physiologische Chemie* **4** (1889), 462–472.

[Leslie 1966] F. M. Leslie, "Some constitutive equations for anisotropic fluids", *Q. J. Mech. Appl. Math.* **19**:3 (1966), 357–370.

[Leslie 1968] F. M. Leslie, "Some constitutive equations for liquid crystals", *Arch. Ration. Mech. An.* **28**:4 (1968), 265–283.

[Nigen and Walters 2002] S. Nigen and K. Walters, "Viscoelastic contraction flows: comparison of axisymmetric and planar configurations", *J. Non-Newton. Fluid Mech.* **102**:2 (2002), 343–359.

[Pieranski and Guyon 1974] P. Pieranski and E. Guyon, "Transverse effects in nematic flows", *Phys. Lett. A* **49**:3 (1974), 237–238.

[Reinitzer 1888] F. Reinitzer, "Beiträge zur kenntniss des cholesterins", *Monatshefte für Chemie* **9**:1 (1888), 421–441.

[Stephen and Straley 1974] M. J. Stephen and J. P. Straley, "Physics of liquid crystals", *Rev. Mod. Phys.* **46**:4 (1974), 617–704.

[Stewart 2004] I. W. Stewart, *The static and dynamic continuum theory of liquid crystals: a mathematical introduction*, CRC, London, 2004.

[Svenšek and Žumer 2002] D. Svenšek and S. Žumer, "Hydrodynamics of pair-annihilating disclination lines in nematic liquid crystals", *Phys. Rev. E* **66**:2 (2002), 021712–021717.

[Tomé and McKee 1994] M. F. Tomé and S. McKee, "GENSMAC: a computational marker and cell method for free surface flows in general domains", *J. Comput. Phys.* **110**:1 (1994), 171–186.

[Tomé et al. 1996] M. F. Tomé, B. Duffy, and S. McKee, "A numerical technique for solving unsteady non-Newtonian free surface flows", *J. Non-Newton. Fluid Mech.* **62**:1 (1996), 9–34.

[Tomé et al. 2002] M. F. Tomé, N. Mangiavacchi, J. A. Cuminato, A. Castelo, and S. McKee, "A finite difference technique for simulating unsteady viscoelastic free surface flows", *J. Non-Newton. Fluid Mech.* **106**:2–3 (2002), 61–106.

[Yoo and Na 1991] J. Y. Yoo and Y. Na, "A numerical study of the planar contraction flow of a viscoelastic fluid using the SIMPLER algorithm", *J. Non-Newton. Fluid Mech.* **39**:1 (1991), 89–106.

Received 13 Aug 2010. Revised 13 Dec 2010. Accepted 10 Jan 2011.

PEDRO A. CRUZ: pedroac@icmc.usp.br
Department of Applied Mathematics and Statistics, University of São Paulo, Av. Trabalhador São-carlense, 400, 13560-970 São Carlos, SP, Brazil

MURILO F. TOMÉ: murilo@icmc.usp.br
Department of Applied Mathematics and Statistics, University of São Paulo, Av. Trabalhador São-carlense, 400, 13560-970 São Carlos, SP, Brazil

IAIN W. STEWART: i.w.stewart@strath.ac.uk
Department Mathematics and Statistics, University of Strathclyde, Livingstone Tower, 26 Richmond street, Glasgow, G1 1XH, United Kingdom

SEAN MCKEE: s.mckee@strath.ac.uk
Department Mathematics and Statistics, University of Strathclyde, Livingstone Tower, 26 Richmond street, Glasgow, G1 1XH, United Kingdom

JOURNAL OF MECHANICS OF MATERIALS AND STRUCTURES

jomms.org

Founded by Charles R. Steele and Marie-Louise Steele

See http://jomms.org for submission guidelines.

JoMMS (ISSN 1559-3959) is published in 10 issues a year. The subscription price for 2011 is US $520/year for the electronic version, and $690/year (+$60 shipping outside the US) for print and electronic. Subscriptions, requests for back issues, and changes of address should be sent to Mathematical Sciences Publishers, Department of Mathematics, University of California, Berkeley, CA 94720–3840.

JoMMS peer-review and production is managed by EditFLOW® from Mathematical Sciences Publishers.

PUBLISHED BY
mathematical sciences publishers
http://msp.org/

A NON-PROFIT CORPORATION

Typeset in LaTeX

Journal of Mechanics of Materials and Structures

Volume 6, No. 7-8 September–October 2011

Special issue

Eleventh Pan-American Congress of Applied Mechanics (PACAM XI)